Characterisation of Low-velocity Penetrating Shrapnel-induced Injuries in Skin Tissue

Tesfaye O. Terefe, Anoop Chawla, Naresh V. Datla

Abstract The rise in global terrorism has led to an increase in blast- and shrapnel-related injuries, particularly affecting the musculoskeletal system, with secondary injuries being the most common. The skin, as the body's first line of defence, is highly vulnerable to penetrating shrapnel. Despite extensive research on the ballistic properties of skin, developing reliable artificial substitutes remains a challenge. This study utilised porcine skin tissue, chosen for its similarity to human skin in younger populations, to simulate human skin for predicting low-velocity shrapnel-induced injuries. Experimental and numerical simulations were conducted for chisel-nosed shrapnel at different velocities. Transmitted forces (TF) were measured using force transducers, with forces reaching up to 400 N at velocity of 76.76 m/s. Damage patterns were analysed using high-speed camera images and compared with numerical simulation results. The energy dissipation ratio was found to be 50.16% at 40.37 m/s and 12.51% at 76.76 m/s, indicating a reduced energy dissipation ratio at higher velocities. The finite element model was validated against experimental data, providing a framework for predicting skin injuries and supporting the development of artificial skin simulants or surrogates.

Keywords Failure mechanisms, injury patterns, low-velocity shrapnel, porcine skin, transmitted force (TF).

I. INTRODUCTION

In recent years, global terrorism has emerged as a significant concern, with terrorist groups carrying out attacks in both urban and rural areas [1]. These groups commonly use weapons like trap bombs, improvised explosive devices (IEDs), and rocket-propelled grenades (RPGs) [2]. As a result, blast-related injuries have become a major cause of hospital admissions [3]. Injuries to the extremities and musculoskeletal system from shrapnel or debris account for up to 50% of combat wounds [4]. These injuries are typically categorized as blast injuries, which are divided into four categories: primary, secondary, tertiary, and quaternary [5]. Among these, secondary blast injuries from penetrating shrapnel or fragments are the most common form of combat-related injuries [6-7]. The severity of shrapnel injuries depends on factors such as the shape, weight and size of the fragments, as well as the distance from the explosion [8].

The penetration of shrapnel into the body at low velocities is influenced by the skin's resistance, with damage occurring through stretching, crushing, tearing or laceration. These processes result in permanent wound tracks and scar tissue formation [9]. Research using post-mortem human subjects (PMHS), animal models, and physical surrogates has explored the ballistic properties of skin to predict the penetration thresholds for various projectiles [10-11]. However, ethical and practical challenges have driven efforts to develop artificial skin substitutes. Despite extensive studies, reliable and reproducible alternatives of skin simulants remain elusive. A finite element (FE) model was developed and validated to study the damage induced in skin simulants by a penetrating stud, revealing that the TF decreased as the approach angle increased from 0° to 30° [12]. Another study developed an FE model of a bionic composite made of skin simulant and gelatin, which demonstrated that the skin retards the shrapnel and effectively reduces damage in the gelatin simulant [13]. While the use of cadaveric tissue in tests will provide valuable data, their use is limited by ethical concerns and scarcity of samples. As a practical alternative, surrogate tissues such as animal skin or synthetic simulants are often used to replicate the behaviour of human skin under shrapnel penetration. For instance, porcine skin is a suitable substitute as it closely resembles human skin, particularly in younger populations [14].

In this study, low-velocity shrapnel-induced skin injuries were investigated experimentally. The shrapnel velocity was varied and the TF was measured while high-speed cameras captured the penetration phenomenon.

T. O. Terefe (tel: +919667773711; e-mail: tesfitti2016@gmail.com) is a PhD scholar and A. Chawla and N. V. Datla are Professors in the Department of Mechanical Engineering, Indian Institute of Technology Delhi, New Delhi, India – 110016.

An FE model replicating experimental conditions was developed and validated against experimental data. The initial findings highlight the potential of porcine skin as a human skin surrogate in assessing shrapnel-induced injuries.

II. MATERIALS AND METHODS

Porcine skin tissue samples were sourced from a local meat supplier within six hours of slaughter; no animals were killed specifically for this study. Tissue was consistently collected from the thigh region, then cleaned, disinfected, and trimmed to about 100 × 100 mm² with a thickness of 3.5±0.25 mm (Fig. 1(a)). The samples were kept moist throughout the testing process to prevent desiccation.

A pneumatic gas gun system, shown in Fig. 1(c), was used to launch the shrapnel in order to simulate low-velocity shrapnel penetration injuries in porcine skin. A nylon sabot guided a chisel-nosed shrapnel and split at the muzzle to release it toward the target. High-speed cameras operating at 20,000 frames per second captured the shrapnel movement and sample deformation and penetration, while two velocity sensors measured the shrapnel speed at approach and after sample perforation. Data from the sensors, synchronised using NI LabVIEW™, enabled analyses of energy loss and skin resistance. High-intensity LED lighting ensured the video was well-illuminated for accurate observations. A custom-designed sample holder, shown in Fig. 1(b), was used to secure the porcine skin tissue during testing. The back frame was mounted on an adjustable base to ensure precise alignment. Two ICP® force sensors (Model: 208C02) were installed to measure the global TF during penetration.

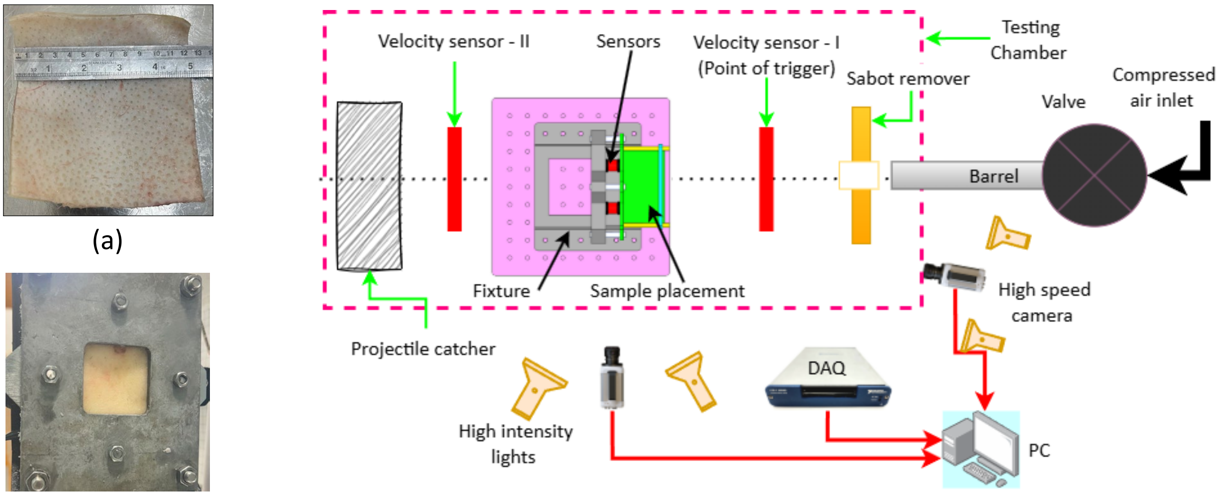

(a) (b) (c)

Fig. 1. (a) Porcine skin tissue sample, (b) fixture with skin sample and (c) schematic of low-velocity gas gun.

Finite element modeling

A 3D model of shrapnel and skin was developed and simulated using LS-DYNA™. The skin was modeled as a 100 × 100 × 3.5 mm^3 block and with mesh refined to 0.5 mm in the contact area and coarser elements at the periphery, as shown in Fig. 2(a) and (b). Shrapnel weighing 6.12 g and featuring a chisel-nosed geometry (Fig. 2(c)) was used for the simulation. The model incorporated material properties, impact velocity, and boundary conditions to replicate the experimental conditions.

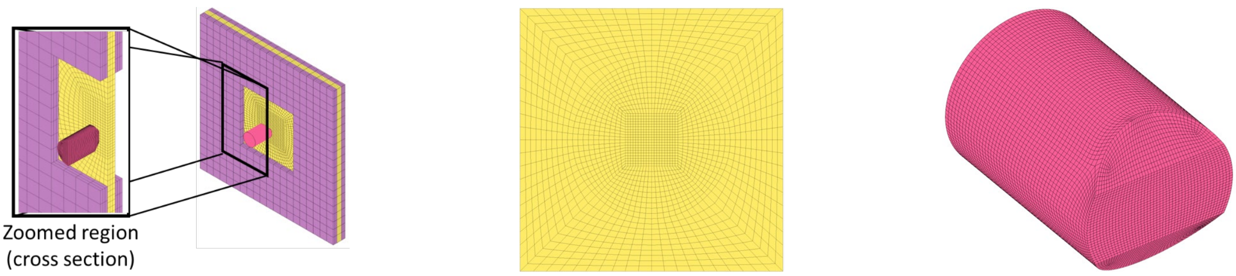

(a) (b) (c)

Fig. 2. (a) 3D FE model geometry, (b) mesh details of skin (front view) and (c) chisel-nosed shrapnel meshing.

Shrapnel-skin interaction was captured using ERODING_SURFACE_TO_SURFACE contact, with Soft = 2 option to account for dissimilarity between materials. A 0.01 hourglass coefficient was applied to minimise numerical errors using viscous hourglass control algorithm. Skin tissue exhibits minimal plastic deformation, undergoing significant deformation prior to failure. Rupture was modeled using a damage criterion based on shear strain failure threshold of 0.6. Element deletion (ADD_EROSION) was employed to simulate material removal once the failure threshold was reached. The skin was secured between rigid frames, with CONTACT_AUTOMATIC_SURFACE_TO_SURFACE defined to prevent undesired motion. This model effectively captured the skin's deformation and erosion during penetration.

Skin tissue shows both the instantaneous elastic response of solids and time-dependent viscous flow. Its hyperelastic quasi-static properties and ability to undergo large deformations are characterised by a strain density function. During impact or penetration, the skin also demonstrates dynamic properties and relaxation which can be modeled using Prony series. This behaviour can be modeled using the general hyperelastic material model in LS-DYNA™ [15]. The Poisson's ratio of skin was considered as 0.48, and other material parameters for porcine skin's hyperelastic [13] and viscoelastic properties [16] are provided in Table I. The shrapnel was modeled as a rigid steel with Young's modulus of 210 GPa and Poisson's ratio of 0.27.

TABLE I

MATERIAL PROPERTIES OF PORCINE SKIN TISSUE

Hyperelastic	E (MPa)	ρ (Kg/m^3)	C_{01} (MPa)	C_{01} (MPa)
	7.642	1030	0.689	0.585
Viscoelastic	G_1	G_2	τ_1	τ_2
	0.0267	0.00807	0.851	40.4

III. EXPERIMENTAL AND SIMULATION RESULTS

Penetration tests were performed on porcine skin tissue using chisel-nosed shrapnel at velocities below 100 m/s. In this study, the term penetration refers to the entry of the shrapnel into the skin, whereas perforation denotes the complete passage of the shrapnel through the skin. The residual velocity of the shrapnel after perforation was measured and compared with numerical simulations conducted under similar conditions. In both experimental and numerical simulations the velocity consistently decreased after perforation. The percentage error in residual velocity was less than 7.75%, indicating a high degree of agreement, as shown in Fig. 3(a). Additionally, Fig. 3(b) compares the TF during chisel-nosed shrapnel penetration at selected impact velocities. The simulation results of TF closely matched the experimental results, where the percentage errors remained below 8%. The force-time history revealed three distinct zones of the penetration process: impact face deformation; penetration; and post-perforation. Zone I involved large deformation of the impact face from point of contact to point 'a', characterised by depression that preceded rupture. At point 'a' the TF reached a peak of 392 N at an impact velocity of 76.76 m/s within 0.05 ms. Zone II was defined from surface rupture onwards and marked by decreased TF, observed from point 'a' to 'b'. High-speed video captured the rapid transition between deformation and rupture phases, emphasising the short time frame within which large deformation and rupture occurred. Zone III was post-perforation in which the shrapnel completely passed through the skin and small fragments or layers of skin were partially or entirely separated from the skin. These zones highlighted the distinct interaction of the shrapnel with the skin tissue.

The effect of shrapnel velocity on the TF in skin tissue was further analysed. The impact velocity (v_{i}), residual velocity (v_{r}) and mass (m_{sh}) of the shrapnel were used to determine the energy absorbed (E_a) by the skin. This can be calculated using Eq. (1), where $\mathrm{E_i}$ and $\mathrm{E_r}$ refer to impact and residual energy, respectively (results given in Fig. 3(c)).

$$\mathrm{E}_a = \mathrm{E_i} - \mathrm{E}_r = m_{\mathrm{sh}}(v_i^2 - v_{\mathrm{r}}^2)/2 \qquad (1)$$

Two distinct damage modes (shown in Fig. 4) were identified during penetration. Mode I corresponds to skin rupture characterised by cross-shaped lacerations on the skin due to the chisel tip. This mode also includes local bulging where the skin is displaced due to compressive forces and uneven pressure distribution. Mode II is the complete shrapnel pass-through, resulting from the combined effects of tensile and shear forces which create perforation in the skin. Another observation is that at low velocity, failure occurs through lateral tearing while higher velocities result in spallation, removing skin parts roughly equal to the shrapnel's diameter.

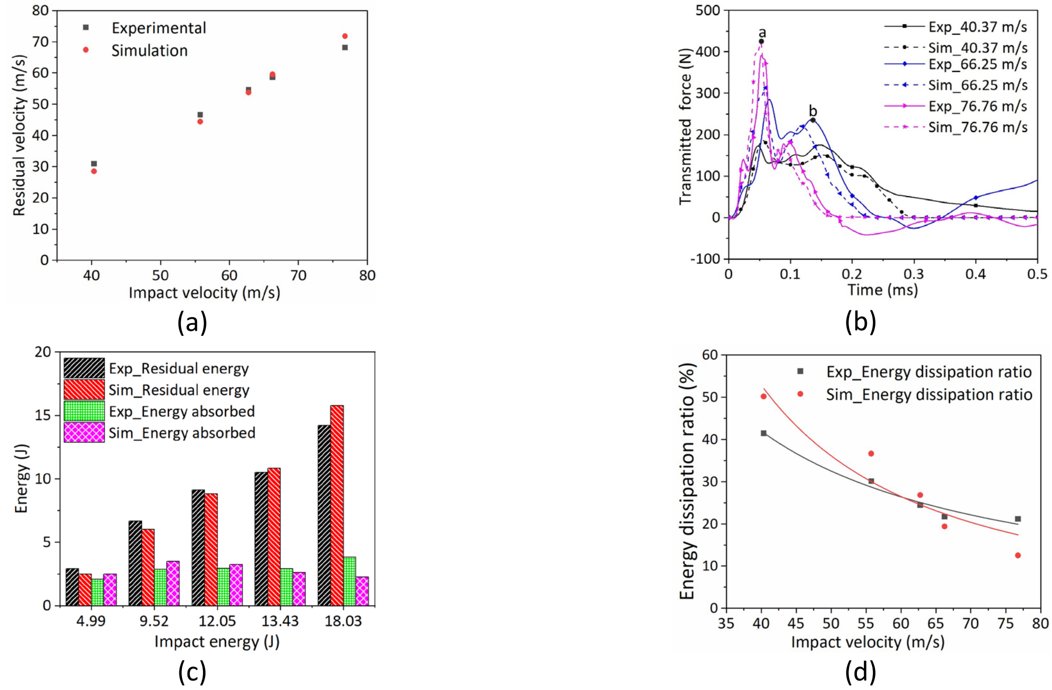

Fig. 3. Comparison of experimental and simulation results: (a) impact vs. residual velocity, (b) transmitted force vs. time, (c) energy absorption analysis, and (d) energy dissipation ratio at different impact velocities.

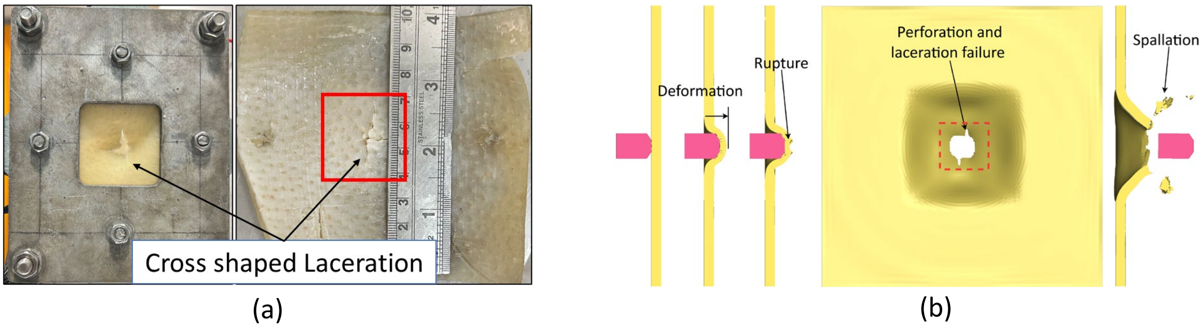

Fig. 4. Deformation and failure patterns observed in skin at 66.25 m/s: (a) experimental, and (b) simulation.

IV. DISCUSSION

The residual velocity and TF predicted in simulations were within 8% of the experimental values. The FE model also effectively captured the dynamics of shrapnel penetration, including energy transfer and the large deformation of the skin tissue. The agreement, evidenced by low percentage error values, confirms the model's reliability in simulating penetration mechanics and behaviour of the skin tissue. Further study of the TF provided insights into injury mechanisms, revealing three distinct zones: impact face deformation; penetration; and post-perforation. Zone I involved large-scale deformation leading to rupture, marked by the TF reaching its maximum. Zone II represented rupture and penetration, where the skin failed to withstand the TF, transitioning into the plastic zone. In Zone III, as the shrapnel passed entirely through the tissue and spallation occurred under the combined effects of tensile and shear forces, the force response decreased rapidly.

As the impact velocity increased, the penetration duration decreased, reflecting the rate at which energy is transferred to the tissue during the penetration. This behaviour indicates rapid energy transfer at higher velocities, resulting in localised and severe damage. The force-time response demonstrated that the maximum TF occurred in Zone I, where a significant portion of kinetic energy was transferred to the skin. This energy transfer aligns with large surface deformation observed in this period. Energy absorption was estimated based on the difference in kinetic energy of the shrapnel before contact and after perforation. The increase in TF with impact velocity highlights its direct correlation with injury severity. Figure 3(c) demonstrates the energy absorption analysis, showing that the energy absorbed by the skin accounted for no more than 40% of the shrapnel total kinetic energy, which decreases with increasing shrapnel velocity. As impact energy increased, the energy dissipation ratio decreased and the skin's ability to withstand penetration was weakened, as shown in Fig. 3(d).

By evaluating TF and residual velocity as validation metrics, the model demonstrated its ability to simulate the dynamics of shrapnel-skin interaction accurately. The percentage errors observed in TF and residual velocity were within acceptable limits, further validating the model's accuracy. The chisel-nosed geometry generated combined tensile and shear stresses, resulting in localised bulging, leading to unique cross-shaped laceration damage patterns and spallation, as shown in Fig. 4.

V. CONCLUSION

This study investigated shrapnel-induced injuries in isolated porcine skin tissue under low-velocity conditions through experimental and numerical approaches. Experimental results were used to validate an FE model by analysing the TF and residual velocity due to shrapnel penetration. Skin injury mechanisms were identified and discussed by correlating experimental observations with simulation outcomes. The FE model gives insight into shrapnel-induced injuries in skin tissue, thereby helping to simulate secondary blast injuries. The findings suggest the use of animal models for understanding skin injury mechanisms, with a need for comparative studies to establish porcine skin as a human surrogate.

VI. ACKNOWLEDGEMENTS

The authors acknowledge the financial support from DRDO Industry Academia Centre of Excellence IIT Delhi (DFTM/03/3203/M/01/JATC).

VII. REFERENCES

[1] Rankin, I. A., Nguyen, T. T., *et al*. (2021) The Injury Mechanism of Traumatic Amputation. *Frontiers in Bioengineering and Biotechnology*, **9**(4): pp. 1–10.

[2] Breeze, J., Newbery, T., *et al*. (2014) The Challenges in Developing a Finite Element Injury Model of the Neck to Predict the Penetration of Explosively Propelled Projectiles. J*ournal of the Royal Army Medical Corps*, **160**(3): pp. 220–225.

[3] Beaven, A. and Parker, P. (2024) Blast Injuries: A Guide for the Civilian Surgeon. *Surgery* (United Kingdom), **42**(7): pp. 461–470.

[4] Ramasamy, A., Hughes, A., *et al*. (2013) The Effects of Explosion on the Musculoskeletal System. *Trauma*, **15**(2): pp. 128–139.

[5] Breeze, J. and Carr, D. J. (2016) Blast Injury Science and Engineering. *Blast Injury Science and Engineering*, A. M. J. Bull, J. Clasper, *et al.,* eds., Springer International Publishing, Cham, pp. 145–153.

[6] Singh, A. K., Ditkofsky, N. G., *et al*. (2016) Blast Injuries: From Improvised Explosive Device Blasts to the Boston Marathon Bombing. *Radiographics*, **36**(1): pp. 295–307.

[7] Terefe, T. O., Chawla, A., *et al*. (2024) Low-Velocity Nail Penetration Response of Muscle Tissue and Gelatin. *Forensic Science International*, **361**(8): p. 112082.

[8] Koser, J., Chirvi, S., *et al*. (2022) Repeated Measures Analysis of Projectile Penetration in Porcine Legs as a Function of Storage Condition. *Journal of Forensic and Legal Medicine*, **90**: p. 102395.

[9] Xiong, M., Qin, B., *et al*. (2019) Experimental Impacts of Less Lethal Rubber Spheres on a Skin-Fat-Muscle Model. *Journal of Forensic and Legal Medicine*, **67**(7): pp. 7–14.

[10] Bir, C. A., Resslar, M., *et al*. (2012) Skin Penetration Surrogate for the Evaluation of Less Lethal Kinetic Energy Munitions. *Forensic Science International*, **220**(1–3): pp. 126–129.

[11] Yoganandan, N., Stemper, B. D., *et al*. (2011) Use of Postmortem Human Subjects to Describe Injury Responses and Tolerances. *Clinical Anatomy*, **24**(3): pp. 282–293.

[12] Imam, S. A., Hughes, A. C., *et al*. (2024) A Finite Element Model for Predicting Impact-Induced Damage to a Skin Simulant. *Scientific Reports*, **14**(1): pp. 1–10.

[13] Wen, C., Liu, S., *et al*. (2022) Investigation of the Retarding Mechanism of Skin on Medium-Low Speed Projectiles in the Bionic Composite Target. *Mechanics of Solids*, **57**(5): pp. 1237–1248.

[14] LeSueur, J., Koser, J., *et al*. (2024) Penetration Thresholds of Porcine Limbs for Low Sectional Density Projectiles in High Rate Impact. *Military Medicine* (in press), **189**: pp. 517–524.

[15] Hallquist, J. (2012) *LS-DYNA Keyword User's Manual, Version 971*, Livermore: Livermore Software Technology Corporation, LSTC.

[16] Payne, T., Mitchell, S., *et al*. (2015) The Evaluation of New Multi-Material Human Soft Tissue Simulants for Sports Impact Surrogates. *Journal of the Mechanical Behavior of Biomedical Materials*, **41**: pp. 336–356.